Letter

Negative Transient Flux in the Near Field of a Subwavelength Source

Xiao Li,[1,2] Pengqi Li,[1,‡] Ming-Hui Lu,[3] Mathias Fink,[4,†] and Guancong Ma[1,*]

[1] *Department of Physics, Hong Kong Baptist University, Kowloon Tong, Hong Kong, China*

[2] *Department of Physics, The Hong Kong University of Science and Technology, Clear Water Bay, Hong Kong, China*

[3] *National Laboratory of Solid State Microstructures & Department of Materials Science and Engineering, Nanjing University, Nanjing, Jiangsu 210093, China*

[4] *Institut Langevin, ESPCI Paris, PSL University, CNRS, 10 rue Vauquelin, Paris, France*

(Received 13 May 2021; revised 3 July 2021; accepted 6 July 2021; published 23 July 2021)

The emission of waves by a small source is a generic wave problem that has long been thought to be well studied. Here, we report the experimental observation that the energy flux of an outgoing sound wave emitted by a deep-subwavelength-sized source can become negative, which indicates the backward flow of energy. Such a negative transient flux exists, even in a homogenous medium, but is only observable in the time domain and in the extreme near field of the source. By wave-impedance analysis, we show that such a phenomenon is fundamentally rooted in the geometry of the wavefield itself and, hence, is generic. Our findings have implications in the time-dependent emission, absorption, and scattering of waves.

DOI: 10.1103/PhysRevApplied.16.L011004

Waves naturally spread out in space, making them an excellent carrier of energy and/or information. Consequently, waves are one of the backbones of modern technologies. As a common practice, wave phenomena are often analyzed in the Fourier domain. Fourier analysis is advantageous in handling steady states, but it inevitably clouds any interesting transient phenomena. A prime example is the time-reversal refocusing of waves [1], which not only focuses wave energy to a specific spot in space but also temporally recompresses the time-reversed codas to a short pulse. Recent investigations also show that temporal modulation of the properties of wave-sustaining media can produce a wide variety of effects that are out of reach for any static media [2–11]. These discoveries have sparked the recent resurgence of revisiting familiar realms in wave physics from the time domain.

In a typical application scenario, a wave is emitted by a source, then travels through some medium before it is detected or absorbed by a receiver. As the first step of this process, the emission of waves by a source is no doubt of great importance, as it underlies the field of antenna designs. The emission process is also fundamentally linked to scattering events because the Huygens-Fresnel principle regards scattering as secondary emission by scatterers under the illumination of incident waves [12]. Hence, the emission problem is also at the center of wave-medium and interface engineering, such as metamaterials and metasurfaces [13–21]. It is therefore a worthy effort to reexamine the emission problem from the temporal perspective. A theoretical study reported the possibility of negative transient flux (NTF) in the vicinity of a point source emitting a spherical wave [22]. This surprising effect has not been verified in observations to date. Here, we investigate, through both theory and acoustic experiments, the transient emission of a wave by a source of deep-subwavelength size in a homogenous medium (air). We report the successful experimental observation that, in the near field of the source, the energy flux of the supposedly outgoing wave can become negative for short durations. This indicates the existence of a backward flow of energy towards the source, as schematically shown in Fig. 1(a). The effect is further explained by using local wave impedance, which reveals its root in the geometry of the wavefield itself. Our demonstration is performed in cylindrical geometry, but the effect is general for emissions in both two dimensions and three dimensions (3D). Although the investigation is carried out with acoustic waves, the NTF is a generic transient phenomenon that also exists for other types of waves.

We begin by considering the time-domain causal Green function for a two-dimensional (2D) acoustic field in a

*phgcma@hkbu.edu.hk

†mathias.fink@espci.fr

‡Present address: School of Physics and Innovation Institute, Huazhong University of Science and Technology, Wuhan 430074, China

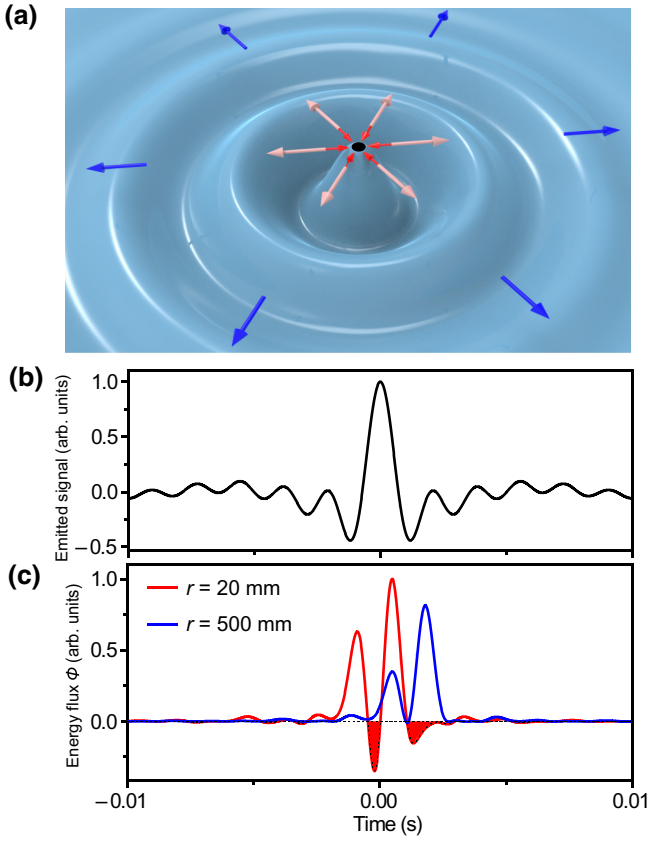

FIG. 1. (a) Schematic drawing showing the emission by a point source (small black dot). In the near field, energy flux can become negative in the time domain, as indicated by red arrows pointing at the source. In the far field, energy flux is always outgoing (blue arrows). (b) Short-pulse signal emitted by the point source covering 100–600 Hz. (c) Energy fluxes, $\phi(t)$, at different distances from the source. NTF is identified and filled with red color. Zero of the time axes coincides with the emission's peak.

homogeneous medium:

$$G(\mathbf{x},t;\mathbf{x}',t') = \frac{1}{2\pi c_0\sqrt{c_0^2(t-t')^2-|\mathbf{x}-\mathbf{x}'|^2}}\times \Theta\left(t-t'-\frac{|\mathbf{x}-\mathbf{x}'|}{c_0}\right), \quad (1)$$

where $\mathbf{x}'$ and t' are the spatial and temporal coordinates of the point source, respectively; c_0 is the speed of sound; and Θ is a step function. We choose polar coordinates for the spatial dimensions. For convenience, the position of the point source is chosen as the origin, so that the entire system is cylindrically symmetric. The emitted temporal signal is given by

$$S(r',t') = s(t')\frac{\delta(r')}{2\pi r'}. \quad (2)$$

The acoustic pressure signal received by a detector at distance r from the source is then given by the Green function [Eq. (1)]:

$$P(r,t) = \int_0^r\int_0^{2\pi}\int_{-\infty}^{+\infty} S(r',t')\ G(r,t;r',t')r'dr'd\theta'dt' = \int_0^{t-\frac{r}{c_0}}\frac{1}{2\pi c_0^2}\left[\frac{s(t')}{\sqrt{(t-t')^2-(r/c_0)^2}}\right]dt'. \quad (3)$$

The velocity field, $\vec{v}$, and pressure field, P, are related by

$$\rho_0\frac{\partial\vec{v}}{\partial t} = -\nabla P, \quad (4)$$

which yields $\vec{v}(r,t) = -\frac{1}{\rho_0}\int\nabla P(r,t)dt$, where ρ_0 is the mass density of the medium. We can then obtain the energy flux, $\vec{\phi}$, at r:

$$\vec{\phi}(r,t) = \oint_L P(r,t)\vec{v}(r,t)d\vec{x} = 2\pi rP(r,t)v(r,t)\hat{r}, \quad (5)$$

where the integration loop, L, is a closed circle with radius r, and $\hat{r}$ denotes the radial unit vector.

Consider the emission of a short pulse, $s(t)$, by the point source in a background of air ($\rho_0 = 1.29$ kg/m^3, $c_0 = 343$ m/s), which has a flat-frequency coverage over $[f_0, f_1]$. We take $f_0 = 100$ Hz and $f_1 = 600$ Hz, as shown in Fig. 1(b). We examine the energy flux, $\phi(t)$, obtained from Eq. (5) at two different positions, $r = 20$ and 500 mm, as shown in Fig. 1(c). It is seen that, for $r = 20$ mm, which is in the near field of the source, the flux can be negative. (The shortest wavelength is 57.2 cm.) According to Eq. (5), a negative-valued flux indicates that the direction of energy propagation is antiparallel to $\hat{r}$, which points away from the source. This means that some emitted energy does not immediately leave the near-field region of the source. Instead, it travels backward. This effect disappears further away from the source ($r = 500$ mm), where the flux is always positive.

We experimentally verify this finding by measuring the temporal emission of a small source. We construct a 2D acoustic waveguide by lifting a square board over the floor [Fig. 2(a)]. A loudspeaker is connected to a small hole with radius $R = 1.5$ mm drilled at the center of the board. The hole is deep subwavelength in size, so that it can be regarded as a point source. Anechoic sponges covered the waveguide's boundaries to minimize reflection. As loudspeakers are usually not effective in generating short sound bursts, we use the pulse-compression technique [23,24] to synthesize the same pulse used in the above discussion. Specifically, we send a relatively long linear chirp signal, $g(t)$, to the loudspeaker by using a waveform generator (Keysight 33500B). Here, $g(t) = \sin[(bt+f_0)t]$

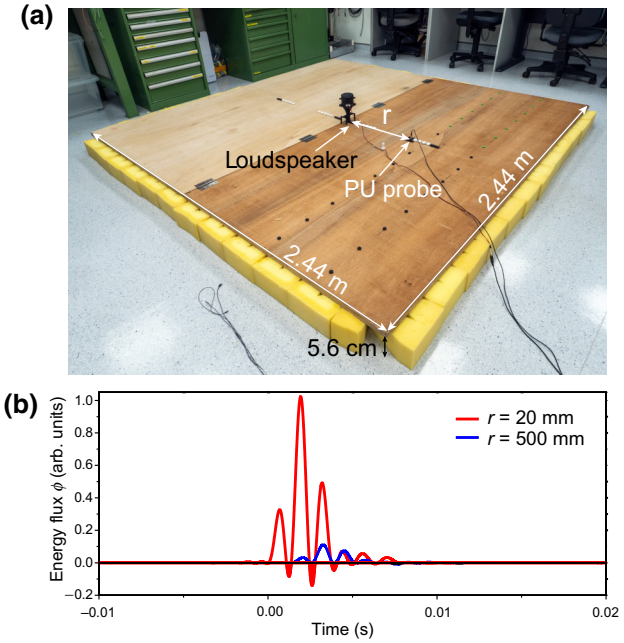

FIG. 2. (a) Experimental setup, which is a 2D waveguide of 5.6 cm thickness. (b) Measured time-dependent energy flux at $r = 20$ and 500 mm. NTF is seen only for $r = 20$ mm.

with $b = (f_1 - f_0)/T$ and $f_0 = 100$ Hz, $f_1 = 600$ Hz, and $T = 0.1$ s being the chirp duration. The detector then also receives a long train of signal $h(r,\ t)$, which is then mathematically cross-correlated with $g(t)$, giving $h'(r,\ t) = g(\tau) \star h(r,\tau) = \int_{-\infty}^{+\infty} g(\tau)h(r,\tau + t)d\tau$, wherein τ is a dummy variable to be integrated over and $\star$ denotes cross-correlation. Since $h(r,t) = \int_{-\infty}^{t-\frac{r}{c_0}} G(r,t;t')g(t')dt'$, $h'(r,\ t) = \int_{-\infty}^{t-\frac{r}{c_0}} G(r,t;t')[g(\tau) \star g(\tau)]dt'$, which contains the autocorrelation of the chirp, $g(\tau)$. The autocorrelation compresses $g(\tau)$ to a sharp pulse as $s(t') = g(\tau) \star g(\tau) = \int_{-\infty}^{+\infty} g(\tau)g(\tau + t')d\tau$, which contains the same Fourier components $[f_0, f_1]$. Hence, $h'(r,\ t)$ is the time-domain impulse response at r, which is what we aim to measure. Then, to obtain the acoustic flux, we use a PU probe (Nanjing Particle Acoustics AVS-PU-1), which simultaneously measures both pressure and velocity of the source field. The PU probe is inserted into small ports at different distances away from the source. The measured signals are recorded on an oscilloscope (Keysight DSO2024A). From the measured results, the time-dependent energy flux can be straightforwardly obtained using Eq. (5). The results are plotted in Fig. 2(b). As the Green function predicts, NTF indeed occurs in the near field of the source.

So far, we have theoretically established and experimentally verified that the energy flux could become negative in the vicinity of a point source. This result emerges in arguably the simplest wave system that consists of a homogeneous medium in the presence of a point source. It does not require any engineering of the medium or any structuring of the source. Hence, it must be an intrinsic property of waves. The reason behind such a phenomenon lies in the geometry of the wavefield itself. To show this, we analyze a monochromatic diverging circular acoustic wave [25]:

$$P = H_0^{(1)}(kr)e^{-i\omega t}, \tag{6}$$

where $H_i^{(1)}(kr)$ is the ith Hankel function of the first kind. The impedance of an outgoing circular acoustic wave is

$$Z = \frac{P}{v} = -Z_0 \frac{iH_0^{(1)}(kr)}{H_1^{(1)}(kr)}, \tag{7}$$

where the velocity, v, is obtained from Eq. (4), and $Z_0 = \rho_0 c_0$ denotes the characteristic impedance of the background medium (air). Equation (7) clearly shows that the impedance is a complex function of kr. We expand Eq. (7) and obtain

$$Z = Z_0 kr\left[\frac{\pi}{2} + i(\gamma - \ln 2 + \ln\ kr)\right] + Z_0 O[(kr)^2], \tag{8}$$

where $\gamma \approx 0.577$ is the Euler-Mascheroni constant. Z becomes purely imaginary when $r \to 0$, with $\mathrm{Arg}(Z) = -\pi/2$, as shown in Fig. 3(a). This result indicates that the pressure, P, and velocity, v, have a local phase mismatch of $-\pi/2$ immediately after emission. Comparing Eqs. (7) and (5), it becomes clear that the cause of the NTF is also the phase difference between P and v, which ultimately results from the circular geometry of the wavefield. On the other hand, the argument of Z approaches zero for large kr. This is expected because, when the wavefront's radius is large compared with the wavelength, locally it becomes indistinguishable from a plane wave. The plane-wave impedance, as defined in Eq. (7), is always a real function. Consequently, the flux of the outgoing wave resumes positive far away from the source.

To verify the above analysis, we also experimentally obtain the argument of Z by using the PU probe to simultaneously measure the phase of P and v in the 2D sound field. Because a phase factor is better defined in a monochromatic wave, we choose to emit a train of sine signals at 700 Hz from the source. The measured results align well with the theoretical prediction [Fig. 3(a)]. Slight deviations at large kr are attributed to the small amount of reflected or scattered waves.

Impedance analysis also implies that the NTF should also exist for a monochromatic wave. This is verified in the results shown in Figs. 3(b) and 3(d). The NTF is clearly seen at $r = 20$ mm, and it exists for every cycle of the sinusoidal wave, further proving that the phase mismatch between P and v is the cause. Again, as the observation point moves away from the source, the amount of NTF diminishes rapidly. The fluxes' behaviors are also shown

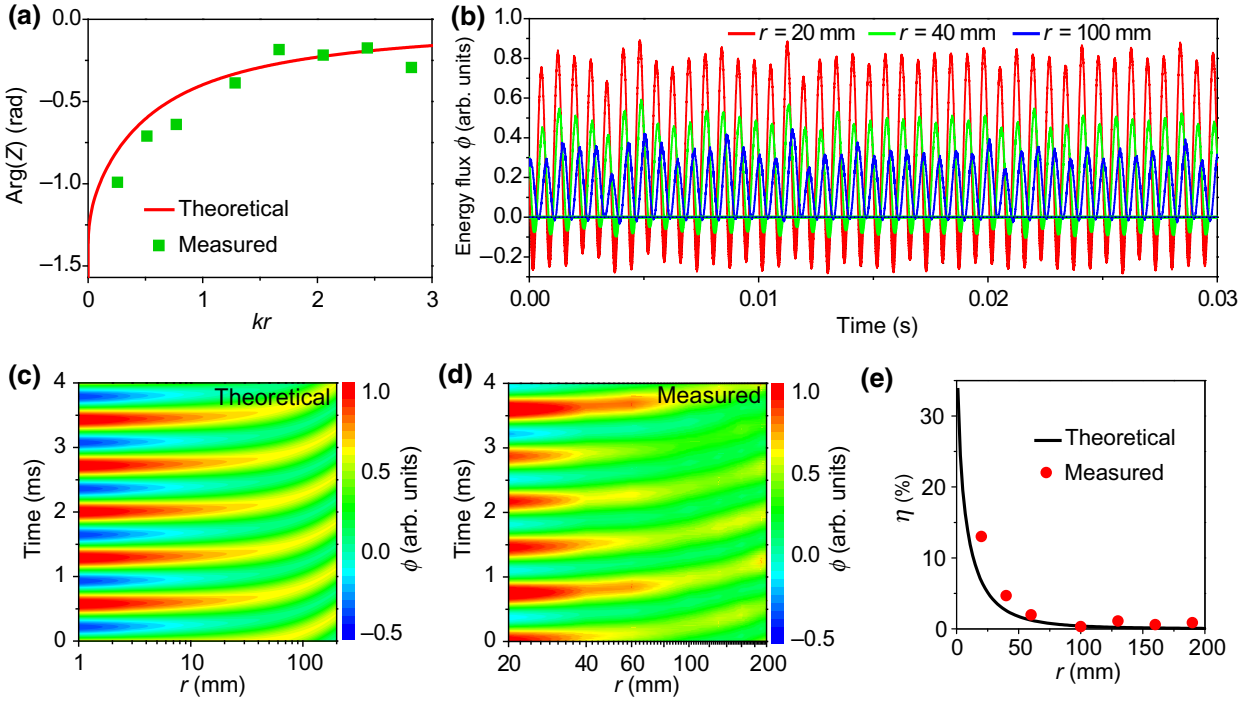

FIG. 3. (a)Argument of impedance as a function of kr. (b) Measured temporal fluxes at different locations. Theoretical (c) and measured (d) energy fluxes as functions of r and t. Data in (d) are an interpolation of measured data on the r axis. (e) Ratio (η) between negative and positive time-averaged fluxes. Emission is a 700-Hz sine train.

in the spatial-temporal map [Figs. 3(c) and 3(d)]. The time average of the negative and positive fluxes can be further obtained, and their ratio, η, is plotted in Fig. 3(e). We also derive the time-averaged net flux, i.e., the sum of negative and positive fluxes:

$$\Phi(r) = \frac{\omega}{2\pi}\int_0^{2\pi/\omega}\oint_{\partial\Omega}\frac{Pv^*}{2}dldt = \frac{2\pi r[J_1(kr)Y_0(kr) - J_0(kr)Y_1(kr)]}{2Z_0} = \frac{2}{kZ_0}, \quad (9)$$

where $\partial\Omega$ denotes some circle centered at the source. The result is positive and is independent of r, which is consistent with the conservation of energy. The positive net flux also indicates that the phase difference between P and v cannot exceed $\pm\pi/2$. This is guaranteed by causality for an emission process, in which the energy must eventually move away from the source.

We note that the NTF does not require any engineering to the source or the medium, which suggests that it is a generic and universal phenomenon observable for waves other than sound. In 3D, an outgoing spherical wave emitted by a source at the origin is $P_{3D} = (e^{ikr}/kr)e^{-i\omega t}$. The corresponding impedance is

$$Z_{3D} = \frac{P_{3D}}{v_{3D}} = Z_0\left(\frac{k^2r^2}{1+k^2r^2} - \frac{ikr}{1+k^2r^2}\right), \quad (10)$$

which is also complex [26]. Arg(Z_{3D}) behaves similarly, with circular-wave impedance, for both $r \to 0$ and r being large, suggesting the existence of the NTF in 3D, which aligns with a previous analysis [22].

Our findings have several implications. First, we recall that evanescent waves can transfer power in directions different from the propagating waves [27–30]. The NTF is related to the complex role of evanescent waves in an emission because it occurs only in the near field of a source. Second, the NTF is observed as the dwelling of energy for a short amount of time before eventually leaving for the far field, which can be a limiting factor of radiation efficiency. Radiation efficiency can be improved by the Purcell effect [31,32] by engineering the local density of states. Our results suggest an alternative route by considering the time dependence of the emission. It further raises the question of whether there is an optimal temporal form for the signal that minimizes the NTF, so that the energy leaves hastily without dwelling in the near field. Another question is how to gain control of the temporal flux by engineering the geometry of the source, the impedance of the surrounding medium, or the source's evanescent components. On the other hand, the existence of the NTF implies a "rebounce" of energy for the focusing of a converging wave, which is the time-reversed process of emission. Such a rebounce prevents the converging wave from carrying all its energy and information to within the near field around the focal spot. Therefore, the rebounce may offer

yet another perspective on the diffraction limit observed for time-reversal refocusing. (Other explanations include the loss of high spatial-frequency components in the form of evanescent waves [33] and interference between incoming and diverging waves [26,34].) Minimizing the flux rebounce can even lead to better designs of absorbers and detectors [26,35]. Lastly, impedance analysis shows that the NTF and its properties are intrinsically underpinned by geometry and causality. This shows a fundamental difference between waves with curvilinear wavefronts and plane waves, since the NTF is absent in the latter. The NTF also cannot exist in one dimension in a homogeneous medium. However, it is possible to engineer the medium to induce the NTF. It may even be possible for some metamaterial to locally induce an equal amount of time-averaged negative and positive fluxes – a scenario that may be useful for wave confinement or energy-storage applications. How to obtain such a medium and what other properties it possesses are fascinating questions for future works.

ACKNOWLEDGMENTS

The authors thank Nanjing Particle Acoustics Technology Co. Ltd. for technical supports with the PU probe. G.M. thanks Ping Sheng for discussions. This work is supported by the Hong Kong Research Grants Council (Grants No. 12302420, No. 12300419, No. 22302718, and No. C6013-18G), the National Natural Science Foundation of China (Grants No. 11922416 and No. 11802256), and Hong Kong Baptist University (Grant No. RC-SGT2/18-19/SCI/006).

[1] M. Fink, From loschmidt daemons to time-reversed waves, Philos. Trans. R. Soc., A **374**, 20150156 (2016).
[2] P. Y. Chen, C. Argyropoulos, and A. Alù, Broadening the Cloaking Bandwidth with Non-Foster Metasurfaces, Phys. Rev. Lett. **111**, 233001 (2013).
[3] R. Fleury, D. L. Sounas, and A. Alù, Subwavelength ultrasonic circulator based on spatiotemporal modulation, Phys. Rev. B **91**, 174306 (2015).
[4] V. Bacot, M. Labousse, A. Eddi, M. Fink, and E. Fort, Time reversal and holography with spacetime transformations, Nat. Phys. **12**, 972 (2016).
[5] L. Zhang, X. Q. Chen, S. Liu, Q. Zhang, J. Zhao, J. Y. Dai, G. D. Bai, X. Wan, Q. Cheng, G. Castaldi, V. Galdi, and T. J. Cui, Space-time-coding digital metasurfaces, Nat. Commun. **9**, 1 (2018).
[6] H. Li, A. Mekawy, and A. Alù, Beyond Chu's Limit with Floquet Impedance Matching, Phys. Rev. Lett. **123**, 164102 (2019).
[7] A. M. Shaltout, K. G. Lagoudakis, J. van de Groep, S. J. Kim, J. Vučković, V. M. Shalaev, and M. L. Brongersma, Spatiotemporal light control with frequency-gradient metasurfaces, Science **365**, 374 (2019).
[8] Y. X. Shen, Y. G. Peng, D. G. Zhao, X. C. Chen, J. Zhu, and X. F. Zhu, One-Way Localized Adiabatic Passage in an Acoustic System, Phys. Rev. Lett. **122**, 094501 (2019).
[9] V. Bruno, C. DeVault, S. Vezzoli, Z. Kudyshev, T. Huq, S. Mignuzzi, A. Jacassi, S. Saha, Y. D. Shah, S. A. Maier, D. R. S. Cumming, A. Boltasseva, M. Ferrera, M. Clerici, D. Faccio, R. Sapienza, and V. M. Shalaev, Negative Refraction in Time-Varying Strongly Coupled Plasmonic-Antenna–Epsilon-Near-Zero Systems, Phys. Rev. Lett. **124**, 043902 (2020).
[10] V. Pacheco-Peña and N. Engheta, Temporal aiming, Light Sci. Appl. **9**, 129 (2020).
[11] V. Pacheco-Peña and N. Engheta, Effective medium concept in temporal metamaterials, Nanophotonics **9**, 379 (2020).
[12] M. Born and E. Wolf, *Principles of Optics: Electromagnetic Theory of Propagation, Interference and Diffraction of Light* (Cambridge University Press, Cambridge, 2019).
[13] H. Chen, C. T. Chan, and P. Sheng, Transformation optics and metamaterials, Nat. Mater. **9**, 387 (2010).
[14] A. V. Kildishev, A. Boltasseva, and V. M. Shalaev, Planar photonics with metasurfaces, Science **339**, 1232009 (2013).
[15] G. Ma, M. Yang, S. Xiao, Z. Yang, and P. Sheng, Acoustic metasurface with hybrid resonances, Nat. Mater. **13**, 873 (2014).
[16] G. Ma and P. Sheng, Acoustic metamaterials: From local resonances to broad horizons, Sci. Adv. **2**, e1501595 (2016).
[17] Y. Li, C. Shen, Y. Xie, J. Li, W. Wang, S. A. Cummer, and Y. Jing, Tunable Asymmetric Transmission via Lossy Acoustic Metasurfaces, Phys. Rev. Lett. **119**, 035501 (2017).
[18] B. Assouar, B. Liang, Y. Wu, Y. Li, J.-C. Cheng, and Y. Jing, Acoustic metasurfaces, Nat. Rev. Mater. **3**, 460 (2018).
[19] Y. Fu, C. Shen, Y. Cao, L. Gao, H. Chen, C. T. Chan, S. A. Cummer, and Y. Xu, Reversal of transmission and reflection based on acoustic metagratings with integer parity design, Nat. Commun. **10**, 1 (2019).
[20] Y. Fu, C. Shen, X. Zhu, J. Li, Y. Liu, S. A. Cummer, and Y. Xu, Sound vortex diffraction via topological charge in phase gradient metagratings, Sci. Adv. **6**, eaba9876 (2020).
[21] W. T. Chen, A. Y. Zhu, and F. Capasso, Flat optics with dispersion-engineered metasurfaces, Nat. Rev. Mater. **5**, 604 (2020).
[22] E. Bossy and R. Carminati, Time-domain radiation and absorption by subwavelength sources, Europhys. Lett. **97**, 34001 (2012).
[23] D. Strickland and G. Mourou, Compression of amplified chirped optical pulses, Opt. Commun. **55**, 447 (1985).
[24] P. Maine, D. Strickland, P. Bado, M. Pessot, and G. Mourou, Generation of ultrahigh peak power pulses by chirped pulse amplification, IEEE J. Quantum Electron. **24**, 398 (1988).
[25] L. L. Beranek and T. Mellow, *Acoustics: Sound Fields and Transducers* (Academic Press, Waltham, 2012).
[26] G. Ma, X. Fan, F. Ma, J. De Rosny, P. Sheng, and M. Fink, Towards anti-causal Green's function for three-dimensional sub-diffraction focusing, Nat. Phys. **14**, 608 (2018).
[27] C. Luo, S. G. Johnson, and J. D. Joannopoulos, All-angle negative refraction in a three-dimensionally

periodic photonic crystal, Appl. Phys. Lett. **81**, 2352 (2002).

[28] C. Luo, S. G. Johnson, J. D. Joannopoulos, and J. B. Pendry, All-angle negative refraction without negative effective index, Phys. Rev. B **65**, 201104 (2002).

[29] B. Hou, J. Mei, M. Ke, W. Wen, Z. Liu, J. Shi, and P. Sheng, Tuning fabry-perot resonances via diffraction evanescent waves, Phys. Rev. B **76**, 054303 (2007).

[30] H. Ge, M. Yang, C. Ma, M. H. Lu, Y. F. Chen, N. Fang, and P. Sheng, Breaking the barriers: Advances in acoustic functional materials, Nat. Sci. Rev. **5**, 159 (2018).

[31] E. M. Purcell, H. C. Torrey, and R. V. Pound, Resonance absorption by nuclear magnetic moments in a solid, Phys. Rev. **69**, 37 (1946).

[32] M. Landi, J. Zhao, W. E. Prather, Y. Wu, and L. Zhang, Acoustic Purcell Effect for Enhanced Emission, Phys. Rev. Lett. **120**, 114301 (2018).

[33] G. Lerosey, J. De Rosny, A. Tourin, and M. Fink, Focusing beyond the diffraction limit with far-field time reversal, Science **315**, 1120 (2007).

[34] J. De Rosny and M. Fink, Overcoming the Diffraction Limit in Wave Physics Using a Time-Reversal Mirror and a Novel Acoustic Sink, Phys. Rev. Lett. **89**, 124301 (2002).

[35] M. Girard, J. A. Millan, and M. Olvera de la Cruz, DNA-driven assembly: From polyhedral nanoparticles to proteins, Annu. Rev. Mater. Res. **47**, 33 (2017).